VOL. 6, NO. 2, FEBRUARY 2011 ISSN 1819-6608
ARPN Journal of Engineering and Applied Sciences


www.arpnjournals.com

STEADY STATE MOTION OF RAIL VEHICLE WITH CONTROLLED CREEP FORCES ON CURVED TRACK

M. Messouci
University M'Hamed Bougara, département de mécanique, FHC, Boumerdès, Algeria
E-Mail: messouci_ma15@live.fr

ABSTRACT

A linear analysis of steady state curve traversing is developed for rail vehicle with wheels coupled with a torsional viscous damper. The governing equations are given and are solved numerically. We consider the equilibrium of the bogie with two wheel sets acted upon by the forces of gravity and the transverse force. The approach is based on providing guidance by creep forces in conjunction with wheel conicity, so that flange contact is normally avoided. It describes the behavior of the vehicle in the curves of different radii. It is, therefore, important to define the characteristics of the torsional damper. It gives the modulus (magnitude) of the moment of friction in the dampers produced by the relative motion of the wheels as well as the bogie yaw, the relative lateral and yaw displacement of the leading and trailing wheel set at each curve track of constant curvature.

Keywords: rail vehicle, steady state motion, curved track, friction, torsional viscous damper, linear analysis.

1. FOREWORD

In every country, a considerable proportion of the total length of track on a rail system is composed of curved tracks. In the curved tracks, excessive longitudinal stiffness in the primary suspension or high centrifugal forces has a detrimental effect on the inscription of the vehicle. They upset the normal guidance assured by the creep forces. This happen because the forces balance is disturbed and demand a greater resultant creep forces than the limiting friction force. As a result the wheel sets slip. The rail vehicle cannot preserve the direction of motion. It skids. The flange contact occurs allowing the flanges forces to restore the equilibrium. The wheels and the rail cannot be safeguarded against accelerated wear. This fact generates a need for a new vehicle design. The vehicle with controlled creep forces is noted for its stability even with a soft longitudinal primary suspension. The technical innovation is to incorporate a torsional viscous damper between wheels of the split up wheel sets. Worthy of notice in the design of rail vehicle is that the smaller the radius of curve, the less should be the longitudinal stiffness or the yaw stiffness in the primary suspension. The vehicle characteristics accepted for calculation in this study are given in the nomenclature. We give and solve equations with account of the design parameters of the damper and the basic characteristics of the curved track (the cant angle and the radius) which are kept constant. We give an overall picture of how the example vehicle behaves through curves and the couple developed in the damper.

2. INTRODUCTION

It must be recognized that in principle the prevailing goal is to design a vehicle so that the creep forces acting on the wheel tread insure guidance in the curve, that is, the flange contact is avoided. Curve traversing under the control of creep forces of an adjusted magnitude has the advantages of minimizing wear of wheel and rail under normal conditions of circulation. It was under these conditions that linear analysis is valid; Boocock developed it [1]. The equations of motion of the vehicle travelling in curves are identical to the equations obtained by alignment unless it appears the functions of forces in the right hand of the equations. The effects of the curvature and the cant of the track are to provide solicitations from outside the vehicle and its static and dynamic stability is therefore the same [2, 3].

In the case of stable traffic at speeds slightly higher than those owing to the forces balance (low cant deficiency), we can neglect in the first approximation, the forces of inertia and damping in respect with suspension forces. Moreover, we believe that the centrifugal forces are small. In these circumstances, we can assume that the roll angles are very small. The vehicle moves at a constant speed along the track, which has a constant centre-line radius and uniform angle of cant.

This study shows the behaviour of the rail vehicle in the curved tracks, its advantages and its limitations. It underlies the determination (the choice and calculation) of the torsional damper as well.

3. VEHICLE ARCHITECTURE

The vehicle used consists of a body, two identical bogies and four-wheel sets. Figure-1 depicts a scheme of one bogie surrounded by the provision of suspensions.

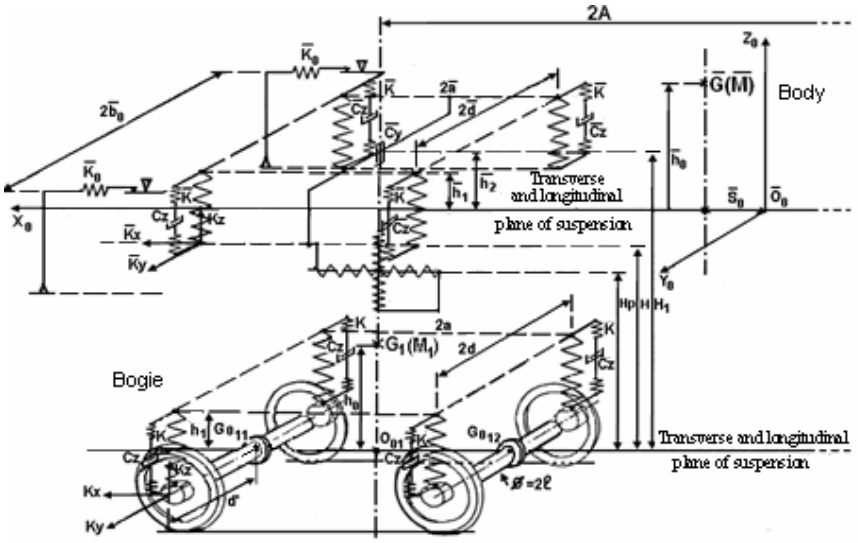

Fig.1. Layout of the suspensions elements of a four wheeled-rail vehicle and its principal parts.

The primary suspension between the bogies and the wheel sets is made by weightless springs in series with rubber pads to damp the noise. Four dampers in parallel with springs complement the suspension. The same goes for the secondary suspension. The body/bogie coupling link allows to the body to perform an oscillatory motion around a cylindrical and longitudinal hinge placed underneath. The lowest end of this coupling link slides in a ball-and-socket joint judiciously located in the bogie frame.

The wheel set consists of two wheels rigidly linked to two semi hollow shafts turning around an inner common axle. A torsional viscous damper connects the two half-hollow shafts. Thus, the rotation of one wheel affects the rotation of the other. The relative rotation between wheels will be more or less constrained depending on the coefficient of resistance value or damping coefficient C_φ of the torsional damper. This consolidation provides an opportunity to the mechanism to return to its equilibrium position: the wheel that climbs up the flange taking the advance on the other wheel causes a rotation of the axle, which tends to bring it to the central position in the track. This constructive feature gives us, in fact, the ability to control the creep forces magnitude generated at the wheels.

4. ROLLING CONTACT THEORY

The Kalker theory of frictional rolling contact allows the evaluation of the contact forces on the wheel [4,5]. He defined a digital process for evaluation these forces. The explanation of creep forces lies in the elastic properties of the wheel and the rail: owing to this elasticity, these two bodies touch along a contact area. This problem was analysed by Hertz. Tangential forces appear in the tiny contact area when the elastic wheel rolls on the elastic rail owing the small deviation from pure rolling of two elastic bodies. Conversely, if we apply external tangential efforts, deviations from continuous rolling can occur. For low values of these movements, there is a pure adhesion over the entire surface of contact: the sliding at the point of contact of the wheel with the rail is negligible and the wheel changes the direction of motion mainly due to elastic deformation. That is, there is a dependence of the elastic deformations on the tangential forces magnitudes in the contact surface between the two bodies: certain constitutive relations derived from the theory of elasticity connect them. If the deviations from pure rolling grow, the bodies touch along a contact area, which permit conditions intermediate between pure adhesion and pure slip. If the deviations are no longer small, the full slipping of the wheel commences. In the contact area, Coulomb's law connects total slip and the tangential forces.

The tangential forces have a limiting value, which is restricted by the friction coefficient of the wheel with the rail surface.

The wheel meets the rail at infinitely large number points of an ellipse. At each point, the Hertz theory allows the determination of the normal pressure in the contact. As the wheel rolls, the deformations increase in the front part of the wheel and diminish at the rear portion. Hence, the elementary reactions in the front area of contact are larger than that in the rear and the line of action of the resultant is displaced with respect to the centre of the ellipse. This resultant builds up moment acting on the wheel. We have to add the reaction moment of the constraint applied to the wheel, which is relative to the spin effect. The connection between the components of deformation and the tangential forces is called the creep-force law, that is, it has the form:
the longitudinal creep force:

$$T_{xj} = - C_{11} \boldsymbol{v}_j \cdot \boldsymbol{x}_0 \quad (1)$$

the lateral creep force :

$$T_{yj} = - C_{22} \boldsymbol{v}_j \cdot \boldsymbol{u}\left(\gamma_j\right) - C_{23} \phi_j \quad (2)$$

the moment:

$$M_j = C_{23}\,\boldsymbol{v}_j \cdot \boldsymbol{u}\left(\gamma_j\right) - C_{33}\,\phi_j \tag{3}$$

In which:
C_{11}, C_{22} and C_{23}, C_{33} are the creep and spin Kalker coefficients. They are functions of the elastic properties (Young modulus E=2.10 x10 ^{11} N.m^{-2}; Poisson's ratio σ = 0.25 for both the wheels and the rail) and of the ratio of the axes of the contact ellipse. These coefficients vary as (wheel load) $^{2/3}$

$\boldsymbol{v}_j$ represents the creepage or creep ratio at the point of contact point I_j,

ϕ_j means the spin at the of contact point I_j,

$\boldsymbol{x}_0$ and $\boldsymbol{u}\left(\gamma_j\right)$ vectors defining the contact plane,

$\boldsymbol{x}_0$ the x-axis pointing along the direction of the steady motion,

$\boldsymbol{u}\left(\gamma_j\right)$ is lying on the contact plane it is perpendicular to the direction of motion.

We will use equations (1), (2) and (3) and we will consider the rail and the wheels absolutely rigid. Therefore, the numerical value of the wheel radius is assumed constant.

Creep forces can be large. Their magnitude is saturated at the limiting friction force. They are able to exert a strong guiding influence during curve traversing.
Creepage or creep ratio.

It is the ratio between the sliding velocity $\boldsymbol{g}$ of the rail to the wheel at the point of contact I_j and the module of the rolling velocity $\boldsymbol{V}$. $\boldsymbol{V}$ is roughly the translation speed of the wheel as a whole.

$$\boldsymbol{v}_j = \frac{\boldsymbol{g}\left(\text{rail} / \text{wheel}, I_j\right)}{\left| V^O \right|\left(I_j\right)} \tag{4}$$

Spin

The spin is connected with the conicity of the wheel. According the definition given by Kalker, the spin is equal to the component ω_N of rate of rotation on the normal axis to the contact plane divided by the module of an average speed of the two bodies in contact. The rail being fixed, the latter is equivalent to the advance speed of the vehicle (Figure-2).

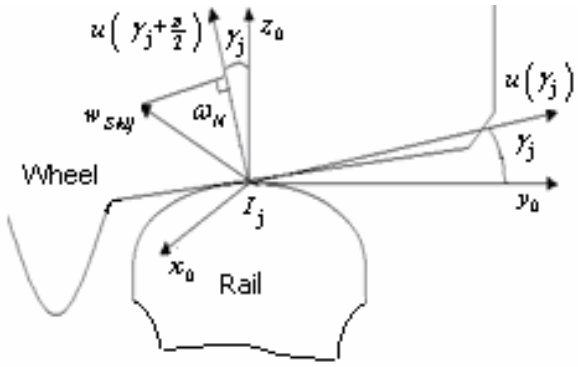

Fig.2. Component of rate of rotation

$$\phi_j = \frac{\omega_{N_j}}{|V|} \tag{5}$$

5. EQUATIONS OF MOVEMENT

It will be noted that the wheel set displacements are specified with respect to the pure rolling line. We show in [1, 3] that the unrestrained wheel sets adopt radial positions in the rack along the pure line rolling in absence of cant deficiency. They are displaced laterally outwards for a pure rolling and for a power dissipated in the torsional damper equal to zero.

The lateral displacement of the pure rolling line from the track centre-line may be written as:

$$y_0 = \frac{e_0 r_0}{R_c \gamma_e} \tag{6}$$

Where

$$\gamma_e = \frac{R\,\gamma_0}{R\text{-}R'}\left[\frac{e_0 + R'\gamma_0}{e_0 - r_0\ \gamma_0}\right] \tag{7}$$

The value of y_0 is positive meaning that the y-axis is directed outwards the curve.

The relative coordinates for the leading bogie may describe the configuration of the vehicle as follows:

α_1^* Yaw displacement of bogie from lie joining wheel sets centres,

y_{11}^* Lateral displacement of the leading wheel set from pure rolling line,

y_{12}^* Lateral displacement of the trailing wheel set from pure rolling line,

α_{11}^* Yaw displacement of leading wheel set from radial lines,

α_{12}^* Yaw displacement of trailing wheel set from radial lines.

A similar set of co-ordinates applies for the trailing bogie.
We obtain the system given in the appendix in which:

$$\vartheta_d = {}^{V^2}\!/_{gRc} - \vartheta_0 \tag{8}$$

$W = \left(\frac{\bar{M}}{4} + \frac{M}{2} + m + \hat{m} \right) g$ Wheel sets load

Kinematics relations bind the roll angle ψ_{ki} to the swing y_{ki}. The motion is studied from geometric standpoint in [6]:

$$\psi_{ki} = \Gamma y_{ki} \text{ with } \Gamma = \frac{\gamma_0}{e_0 - r_0 \gamma_0} \quad (9a, b)$$

In addition, the vertical position of the wheel set inertia centre is given by the geometry study:

$$z_{ki} = f(y_{ki}, \alpha_{ki}) \text{ or } z_{ki} = \xi \frac{y_{ki}^2}{2} - \varepsilon_0 \gamma_0 \frac{\alpha_{ki}^2}{2} \quad (10a, b)$$

with

$$\chi = \frac{e_0}{e_0 - r_0 \gamma_0} \; ; \varepsilon_0 = e_0 - (R - 2r_0)\gamma_0 \quad (11a, b)$$

$$\xi = \frac{1}{R - R'} \left\{ \frac{e_0 + R\gamma_0}{e_0 - r_0 \gamma_0} \right\} \; ; \Gamma = \frac{\gamma_0}{e_0 - r_0 \gamma_0} \quad (12a, b)$$

It is shown in [1, 2] that the equations for the leading and trailing bogies and vehicle body may be decoupled. The vehicle body lies approximately tangential to the track at its mid-length.

The motion can be described in terms of only nine equations, which are applicable for both leading and trailing bogies. The relative lateral displacements of the vehicle body and the bogie frame are given in [1]. The remaining displacements are yielded by nine equations given in the appendix.

5.1 Forces acting in the vehicle

The major lateral forces and couples acting on the various mass elements of the vehicle given in [1] are:
- the centrifugal forces,
- the gravitational forces due to track cant,
- the suspensions forces:

-the secondary yaw suspension couple $\bar{C}$ in equation (A.1) is:

$$\bar{C} = -2\bar{K}_x \bar{d}^2 \left[\frac{\bar{A}}{R_c} - \alpha_1^* + \left(y_{11}^* - y_{12}^* \right) / 2a \right] \quad (13)$$

-the primary suspension exerts the following yaw couple C on the leading wheel set; given in equation (A.4):

$$C = -2K_x d^2 \left[\frac{a}{R_c} + \alpha_1^* - \alpha_{11}^* + \left(y_{11}^* - y_{12}^* \right) / 2a \right] \quad (14)$$

In addition to these forces, the particular longitudinal and lateral creep forces of the leading wheel set can be calculated from the following relations (15, 16 17 and 18). With appropriate indices, they are applicable to the trailing wheel set. They are the same than for a straight line except the terms relating the curvature effect [3].

$$\nu_1 = -\frac{r_0 \dot{\varphi}_{111}}{V} \boldsymbol{x}_0 + \left(\frac{\chi \dot{y}}{V} - \alpha_{11}^* \right) \boldsymbol{u}(\gamma_1) \; ; \quad (15)$$

$$\nu_2 = -\frac{r_0 \dot{\varphi}_{112}}{V} \boldsymbol{x}_0 + \left(\frac{\chi \dot{y}}{V} - \alpha_{11}^* \right) \boldsymbol{u}(\gamma_2) \; ; \quad (16)$$

$$\phi_1 = -\frac{\gamma_0 \dot{\varphi}_{111}}{V} - \frac{\gamma_e}{R\gamma_0 r_0} y_{11} + \frac{\gamma_0 \gamma_e}{r_0^2} y_{11}^* - \frac{\gamma_0}{r_0} - \frac{\gamma_0 e_0 \gamma_e}{R_c r_0^2} y_{11} - \frac{1}{R_c} \; ; \quad (17)$$

$$\phi_2 = \frac{\gamma_0 \dot{\varphi}_{112}}{V} - \frac{\gamma_e}{R\gamma_0 r_0} y_{11} + \frac{\gamma_0 \gamma_e}{r_0^2} y_{11}^* + \frac{\gamma_0}{r_0} + \frac{\gamma_0 e_0 \gamma_e}{R_c r_0^2} y_{11} - \frac{1}{R_c} \quad (18)$$

Where $(\cdot)$ is the usual time derivative
y_{ki} lateral displacement from track centre line

In curvilinear motion, the inner wheels with respect to the centre of turn are unloaded under the gyroscopic and centrifugal forces upon the wheel set. The outer wheels bear greater load. The change ΔT_Z can be calculated by the formula (19).

$$\Delta T_Z = \frac{1}{2e_0} \left(W \vartheta_d r_0 + \frac{m \rho_y^2 V^2}{R_c r_0} \right) \quad (19)$$

Due to a small change as compared with the weight load and for simplicity, the numerical values of the Kalker coefficients are assumed equal for the right and left hand wheels of the wheel set. This difference in wheel loads causes an increase in longitudinal creep coefficient at the lighter-loaded wheel and a decrease at the heavier-loaded wheel until the associated creep forces are equal in magnitude but opposite in sign.

Let us write the equations of force moments acting upon each wheel of the leading wheel set. For simplicity, let us disregard the spin effect. Therefore, as given in equations (A.6) and (A.7) we have:

$$C_{11} \frac{r_0^2}{V} \dot{\varphi}_{111} = C_\varphi \left(\dot{\varphi}_{112} - \dot{\varphi}_{111} + 2V \frac{\gamma_e}{r_0^2} y_{11} \right) \quad (20)$$

$$C_{11} \frac{r_0^2}{V} \dot{\varphi}_{112} = C_\varphi \left(\dot{\varphi}_{111} - \dot{\varphi}_{112} - 2V \frac{\gamma_e}{r_0^2} y_{11} \right) \quad (21)$$

The longitudinal forces $C_{11} \frac{r_0}{V} \dot{\varphi}_{111}$ of the outer wheel and $C_{11} \frac{r_0}{V} \dot{\varphi}_{112}$ of the inner wheel are numerically equal but are opposite in sign. They are able to exert a strong guiding influence during curve traversing.

From these equations, we may deduce that $\dot{\varphi}_{kij}$ can appear only with $y_{ki.}$ The ability to turn is a result of lateral slip from pure rolling line.

We can show from the equations 20 and 21 that $\dot{\varphi}_{111}$ is positive for $y_{11}>0$. This case always happens with the leading wheel sets.

Similarly, we can show from equations A.8 and A.9 that $\dot{\varphi}_{121}$ is negative for $y_{12}<0$ with $\left|\dot{\varphi}_{121}\right| < \left|V\frac{\gamma_e}{r_0^2}y_{12}\right|$.

This case may happen with the training wheel set for $\gamma_e \geq 0.2$ and a small radius *Rc* Tables (4, 5). That is, the couple developed by the longitudinal creep forces is then opposite to the leading wheel set one.

Curved tracks with a high radius

For these curves, we can keep the vehicle running at high speed.

There is no need for such curves for high longitudinal creep forces to strain the yaw soft suspension springs through small angles of ±a / R_C. See the equations (A.4) and (A.5) in the appendix.

Curved tracks with a small radius

There is a need for greater longitudinal forces so to strain the yaw soft suspensions springs through rather higher angles ±a / R_C. See equations (A.4) and (A.5).

Centrifugal forces

The action of centrifugal force may cause the wheels to slip in a transverse direction. The unbalanced centrifugal forces can be reacted by lateral creep forces.

5.1.1 Remarks

The linear dependence of the equations (1, 2 and 3) is valid only if the wheel slip and flange contacts are avoided. The bonds of the linear theory will be taken to slip condition [2; 3].

For a wheel affected by the longitudinal force T_x and the transverse force T_y, the resultant reaction R appears in the contact area.

$$R=(T_X^2+T_Y^2)^{1/2} \quad (22)$$

$T_{x \text{ and }} T_y$ can appear only if the wheel is acted upon by the third component: the normal reaction of the rail to the load.

The following condition should be observed for a wheel to move without horizontal and transverse slip:

$$R \leq \mu T_Z \quad (23)$$

Where μ is the coefficient of friction between wheel and rail ; T_Z is the wheel load. If this inequality is violated, the vehicle skids and looses its steer ability. In conformity with the above formula, the following condition is to be observed for a wheel to roll without slipping:

$$T_Y \leq (\mu^2 T_Z^2 - T_X^2)^{1/2} \quad (24)$$

Thus, the greater the force $\mu\ T_Z$ and the smaller the force T_X, the higher will be the transverse force that can be applied to wheel without causing it to slip. Higher proportion of the resultant reaction force is then available to equilibrate unbalanced centrifugal forces.

6. RESULTS AND DISCUSSIONS

The tabulated data (Table-1) are taken from the graph of dependence of the critical speed on the coefficient C_φ for three values of γ_e (Figure-3) [3,7].

Table-1. Admissible value of C_φ with the speed.

V (m.s^{-1})	111	70	50	35
C_φ (N.m.s.rad^{-1})	4500	3 10^4	5 10^5	5 10^5

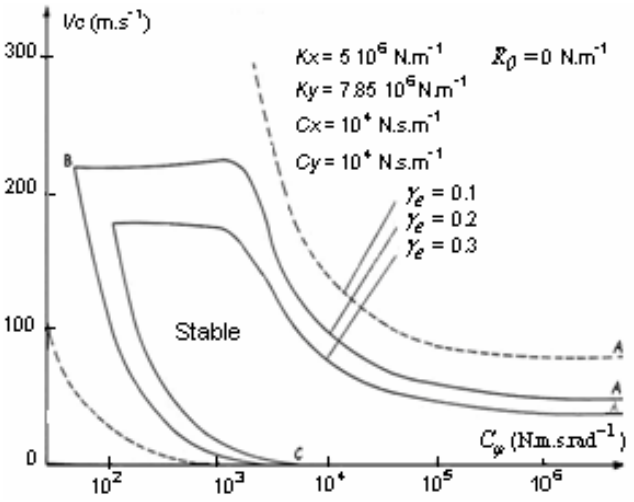

Figure-3. Dependence of the critical speed on *Cφ* for 3 values of γe and a particular value of *Kx, Ky, Cx* and *Cy*.

According to this Figure, we must enslave the damping effect between wheels at to desired speed of the vehicle so to exceed the speed practiced to day. The key is to reduce the damping coefficient as speed increases. This reduction must be highest so to offset the negative effect in performance of a strong γ_e. As regard, dynamic behaviour the wheels provided with adjustable torsional coefficient allows greatest critical speeds with a soft primary suspension. This is an advantage compared to the wheels made integral with a common axle or to the wheels made independent on a common axle.

The results given in Tables 2, 3, 4 and 5 with three values of γ_e and three radius prompt the conclusions that the longitudinal creep forces arising from the displacements y_{ij}^* align the wheel sets correctly almost in a radial position by straining the soft yaw suspension and so enable the necessary lateral creep force to be generated.

All these results hold with no wheel set sipping for the case μ =0.27.

The cant angle track is set equal to 6°. It is lesser than the critical cant angle for toppling conditions.

Table-2. Results for Rc = 10 km and V = 111 m.s$^{-1.}$

	γ_e = **0.1**	γ_e = **0.2**	γ_e = **0.3**
α^* rad	-.8760 10^{-4}	-.6348 10^{-4}	-.4956 10^{-4}
α^* rad	.3150 10^{-2}	.1321 10^{-2}	.7894 10^{-3}
y^*_{12} m	.2155 10^{-2}	.6248 10^{-3}	.2590 10^{-3}
α^*_{11} rad	.1234 10^{-4}	-.4549 10^{-5}	-.8835 10^{-5}
α^*_{12} rad	-.1658 10^{-3}	- .1327 10^{-3}	-.1141 10^{-3}
g_1 rad.s^{-1}	.2587	.2247	.2058
g_2 rad.s^{-1}	.1770	.1063	.6755 10^{-1}
C_1N.m	.1164 10^4	.1011 10^4	.9263 10^3
C_2N.m	.7964 10^3	.4784 10^3	.3040 10^3
$C\varphi$ = 4500 (N.m.s.rad^{-1})		ϑ_d =0.02	

Table-3. Results for Rc = 2 km and V = 70 m.s^{-1}.

	γ_e = **0.1**	γ_e = **0.2**	γ_e = **0.3**
α^* rad	-.3503 10^{-3}	-.2492 10^{-3}	-.1998 10^{-3}
y^*_{11} m	.6003 10^{-2}	.2404 10^{-2}	.1415 10^{-2}
y^*_{12} m	.3203 10^{-2}	.7367 10^{-3}	.2463 10^{-3}
α^*_{11} rad	-.3745 10^{-3}	-.4118 10^{-3}	-.405110^{-3}
α^*_{12} rad	-.107210^{-2}	-.883710^{-3}	-.779010^{-3}
g_1 rad.s^{-1}	.1723	.1501	.1397
g_2 rad.s^{-1}	.9195 10^{-1}	.4603 10^{-1}	.2436 10^{-1}
C_1N.m	.5170 10^4	.4504 10^4	.4190 10^4
C_2N.m	.2759 10^4	.1381 10^4	.7307 10^3
$C\varphi$ =3 10^4 (N.m.s.rad^{-1})		ϑ_d =.14	

Table-4. Results for Rc =1km and V = 50 m.s^{-1}.

	γ_e = **0.1**	γ_e = **0.2**	γ_e = **0.3**
α^* rad	-.4615 10^{-3}	-.2835 10^{-3}	-.2093 10^{-3}
y^*_{11} m	.6097 10^{-2}	.2270 10^{-2}	.1287 10^{-2}
y^*_{12} m	.1620 10^{-2}	-.5066 10^{-4}	-.2158 10^{-3}
α^*_{11} rad	-.2752 10^{-3}	-.3869 10^{-3}	-.3982 10^{-3}
α^*_{12} rad	-.1204 10^{-2}	-.9361 10^{-3}	-.8043 10^{-3}
g_1 rad.s^{-1}	.1694 10^{-1}	.1450 10^{-1}	.1351 10^{-1}
g_2 rad.s^{-1}	.4510 10^{-2}	.3154 10^{-3}	.2260 10^{-2}
C_1N.m	.8471 10^4	.7251 10^4	.6757 10^4
C_2N.m	.2255 10^4	.1577 10^3	.1130 10^4
$C\varphi$ = 5 10^5 (N.m.s.rad^{-1})		ϑ_d = .15	

Table-5. Results for Rc = 1km and V = 35 m.s^{-1}.

	γ_e = **0.1**	γ_e = **0.2**	γ_e = **0.3**
α^* rad	-.3481 10^{-3}	-.1632 10^{-3}	-.9211 10^{-4}
y^*_{11} m	.5567 10^{-2}	.2008 10^{-2}	.1128 10^{-2}
y^*_{12} m	.5182 10^{-3}	-.569010^{-3}	-.5264 10^{-3}
α^*_{11} rad	.3310 10^{-3}	.1491 10^{-3}	.9858 10^{-4}
α^*_{12} rad	-.3905 10^{-3}	-.2036 10^{-3}	-.1317 10^{-3}
g_1 rad.s^{-1}	.1512 10^{-1}	.1248 10^{-1}	.1150 10^{-1}
g_2 rad.s^{-1}	.1411 10^{-2}	.3535 10^{-2}	.5359 10^{-2}
C_1N.m	.7558 10^4	.6240 10^4	.5750 10^4
C_2N.m	.7054 10^3	.1768 10^4	.2679 10^4
$C\varphi$ = 5 10^5 (N.m.s.rad^{-1})		ϑ_d = .02	

Where $C_1 = C_\varphi g_1$ (25)

$$g_1 = \left| \dot{\varphi}_{112} - \dot{\varphi}_{111} + 2V \frac{\gamma_e}{r_0^2} y^*_{11} \right| \quad (26)$$

and $C_2 = C_\varphi g_2$ (27)

$$g_2 = \left| \dot{\varphi}_{122} - \dot{\varphi}_{121} + 2V \frac{\gamma_e}{r_0^2} y^*_{12} \right| \quad (28)$$

6.1 Cant deficiency

The calculations show that it is possible to travel faster. The restrictions will appear first from the requirements of comfort before those of safety traffic. An idea of the change in ϑ_d is given in Tables 4 and 5.

A higher cant deficiency causes the bogie to yaw more and inwards and to produce counterbalancing lateral creep forces.

6.2 Wheel sets displacements

The leading wheel set is always displaced laterally outwards but the trailing wheel set may be displaced inwards or outwards (Tables 4 and 5). The trailing wheel set outward displacement appears only with the smaller conicity in curved tract with a small radius and with all the conicity values for the higher track radius (Table-2). The value of these deviations is too small even with a higher speed.

Therefore, there is no need for a large clearance between the wheel set and the track.

6.3 Effective conicity

The lateral displacement and the yaw of both the bogie frame and the wheel set are sensitive to variation of conicity. There numerical values are less with a higher

conicity. The reason is that the absolute value of the creep coefficients is higher. It is known that the great conicity promotes good curving performance [1].

6.4 Yaw displacement

The Tables 2 to 5 indicate that the wheel sets depart more and more from radial alignment as both *R*c and the speed are increased. The larger yaw angles correspond to the smaller effective conicity. From Tables 4 and 5 the wheel sets yaw in phase at the speed of 50m.s^{-1} and yaw in anti-phase at 35m.s^{-1}. It follows from the comparison of Tables (4 and 5) with the reduction of the speed the leading wheel set yaws outwards. That is, the leading wheel set steer slightly leftwards to turn the rail vehicle rightwards. In addition, its lateral force (not given) is higher. Therefore, the leading wheel set is the first to slip during curve traversing with radius smaller than 1km.

6.5 Damper

The best design is the one that keeps the overall size and mass of the torsional damper to a minimum. It has to be designed so to ensure good operating ability, better reliability and a longer service life. The lock is then of prime importance. The couple developed by the damper is equal to 8471 N.m in a radius tract of 1km; it corresponds to g_1 = 0.1512 10^{-1} rad.s^{-1} and $\gamma_e = 0.1$ (Table-4). It is equal to 1164 N.m for the radius of 10 km with g_1 = 0.2587 rad.s^{-1} and $\gamma_e = 0.1$ (Table-2). Comparing the couple developed at 10 km radius curved track to the couple developed at 1 km radius curved track, it can be clearly seen that the couple at 1km is roughly seven times larger. Besides, the critical speed is relatively constant for the high value of c_φ (Figure-3) and each wheel set behaves as a single piece in straight line.
An electromagnetic power clutch may be used.

6.6 Damping coefficient

With the increase of c_φ the lateral displacement of the leading wheel set is more and more reduced. The value of c_φ has to lie within a margin so the loss of stability can be preserved and safe motion ensured.

6.7 Remarks

The minimum curve radius, which can be negotiated without slip at any cant deficiency, is 1 km for the assumed coefficient of friction $\mu = 0.27$

There is a necessity to lock the liaison between the wheels so to cut down on the torsional damper failures.

The vehicle can be made to travel as faster as possible in the track with a small curvature and to slow down in the greatest with locked wheel sets. The vehicle speed average will be still at a high level.
The speed increase imposes high demands on the braking systems.

For the so-called "TGV", the slip of the wheels cannot be avoided for a curved track whose radius is below 8 km.

When the rail vehicle moves, the situation in the line incessantly changes which calls for increased attention on the part of the driver and a constant readiness to change c_φ value.

7. CONCLUSIONS

We gave an overview of the theoretical curve behaviour of the vehicle with springs stiffness *Kx* = 5. MN.m^{-1} and *Ky* = 7.85 MN.m^{-1} at the primary suspension. This calculation puts the problem of selection and order of magnitudes characteristics of the torsional damper. Moreover, it shows that the trajectory of a small radius is possible. Because the improved registration of the wheel sets in the track, the risk of derailment and the aggressiveness in view of the track are smaller. It can therefore travel faster through a biggest distance than the "TGV" for which the average course is 200 000 km. It may supplant all the other rail vehicles.

REFERENCES

[1] D. Boocock. 1969. Steady-state motion of railway vehicles on curved tract. Journal Mechanical Engineering Science. Vol. 6.

[2] R. Joly. 1983. Stabilité transversale et confort vibratoire en dynamique ferroviaire. Thèse de doctorat d'Etat, Université de Paris VI.

[3] M. Messouci. 1987. Performances d'un véhicule ferroviaire muni de roues à pseudo glissement contrôlé, stabilité transversale en alignement et inscription en courbe, Thèse, ENSAM, Paris.

[4] J.J. Kalker. 1967. On the rolling contact of two elastic bodies in the presence of dry friction. Doctorate Thesis. Delft University.

[5] J.J. Kalker. 1979. Survey of Wheel-Rail Rolling Contact Theory. Vehicle System Dynamics. Vol. 5, pp. 317-358.

[6] A.D. Pater. 1963. Précis de la théorie de l'interaction entre la voie et le véhicule du chemin de fer. Document ORE UTRCHT.

[7] M. Messouci. 2009. Lateral stability of rail vehicles-A Comparative study. ARPN Journal of Engineering and Applied Sciences. 4(3): 13-27.

Appendix

α_1^* Equation (A.1)

$$2\left(\bar{K}_x\bar{d}^2+2K_xd^2+2K_ya^2\right)\alpha_1^*+\left(\bar{K}_x\frac{\bar{d}^2}{a}+2K_x\frac{d^2}{a}\right)y_{11}^*-\left(\bar{K}_x\frac{\bar{d}^2}{a}+2K_x\frac{d^2}{a}\right)y_{12}^*-2K_xd^2\alpha_{11}^*$$
$$-2K_xd^2\alpha_{12}^*=\bar{K}_x\bar{d}^2\frac{\bar{A}}{R_C}$$

y_{11}^* Equation (A.2)

$$-2K_ya\alpha_1^*+\left(W\xi-2C_{23}\gamma_e\left(\frac{\chi}{R\gamma_0r_0}-\frac{\gamma_0\chi}{r_0^2}\right)\right)y_{11}^*-2C_{22}\chi\alpha_{11}^*-C_{23}\frac{\gamma_0\chi}{V}\left(\dot{\varphi}_{111}-\dot{\varphi}_{112}\right)=W\vartheta_d-W\xi y_0$$
$$+2C_{23}\frac{\gamma e}{R\gamma_0r_0}y_0+2C_{23}\frac{\chi}{R_C}$$

y_{12}^* Equation (A.3)

$$2K_ya\alpha_1^*+\left(W\xi-2C_{23}\gamma_e\left(\frac{\chi}{R\gamma_0r_0}-\frac{\gamma_0\chi}{r_0^2}\right)\right)y_{12}^*-2C_{22}\chi\alpha_{12}^*-C_{23}\frac{\gamma_0\chi}{V}\left(\dot{\varphi}_{121}-\dot{\varphi}_{122}\right)=W\vartheta_d-W\xi y_0$$
$$+2C_{23}\frac{\gamma_e}{R\gamma_0r_0}y_0+2C_{23}\frac{\chi}{R_C}$$

α_{11}^* Equation (A.4)

$$-2K_xd^2\alpha_1^*+\left(-K_x\frac{d^2}{a}-2C_{33}\gamma_e\left(\frac{1}{R\gamma_0r_0}-\frac{\gamma_0}{r_0^2}\right)\right)y_{11}^*+K_x\frac{d^2}{a}y_{12}^*+\left(2C_{23}+2K_xd^2-W\gamma_0\varepsilon_0\right)\alpha_{11}^*$$
$$-\left(C_{33}\frac{\gamma_0}{V}-C_{11}\frac{e_0r_0}{V}\right)\dot{\varphi}_{111}+\left(C_{33}\frac{\gamma_0}{V}-C_{11}\frac{e_0r_0}{V}\right)\dot{\varphi}_{112}=2C_{33}\gamma_e\frac{1}{R\gamma_0r_0}y_0+2C_{23}\frac{1}{R_C}+2K_xd^2\frac{a}{R_C}$$

α_{12}^* Equation (A.5)

$$-2K_xd^2\alpha_1^*-K_x\frac{d^2}{a}y_{11}^*+\left(K_x\frac{d^2}{a}-2C_{33}\gamma_e\left(\frac{1}{R\gamma_0r_0}-\frac{\gamma_0}{r_0^2}\right)\right)y_{12}^*+\left(2C_{23}+2K_xd^2-W\gamma_0\varepsilon_0\right)\alpha_{12}^*$$
$$-\left(C_{33}\frac{\gamma_0}{V}-C_{11}\frac{e_0r_0}{V}\right)\dot{\varphi}_{121}+\left(C_{33}\frac{\gamma_0}{V}-C_{11}\frac{e_0r_0}{V}\right)\dot{\varphi}_{122}=2C_{33}\gamma_e\frac{1}{R\gamma_0r_0}y_0+2C_{23}\frac{1}{R_C}-2K_xd^2\frac{a}{R_C}$$

$\dot{\varphi}_{111}$ Equation (A.6)

$$\left(-2C_\varphi V\frac{\gamma_e}{r_0^2}-C_{33}\gamma_e\left(\frac{\gamma_0^2}{r_0^2}-\frac{1}{Rr_0}-\frac{e_0\gamma_0^2}{R_cr_0^2}\right)\right)y_{11}^*-C_{23}\gamma_0\alpha_{11}^*+\left(C_\varphi+C_{11}\frac{r_0^2}{V}+C_{33}\frac{\gamma_0^2}{V}\right)\dot{\varphi}_{111}-C_\varphi\dot{\varphi}_{112}=$$
$$-C_{33}\gamma_0\gamma_e\left(\frac{1}{R\gamma_0r_0}+\frac{\gamma_0e_0}{R_cr_0^2}\right)y_0-C_{33}\left(\frac{\gamma_0}{R_C}+\frac{\gamma_0^2}{r_0}\right)$$

$\dot{\varphi}_{112}$ Equation (A.7)

$$\left(-2C_\varphi V\frac{\gamma_e}{r_0^2}+C_{33}\gamma_e\left(\frac{\gamma_0^2}{r_0^2}-\frac{1}{Rr_0}+\frac{e_0\gamma_0^2}{R_cr_0^2}\right)\right)y_{11}^*+C_{23}\gamma_0\alpha_{11}^*-C_\varphi\dot{\varphi}_{111}+\left(C_\varphi+C_{11}\frac{r_0^2}{V}+C_{33}\frac{\gamma_0^2}{V}\right)\dot{\varphi}_{112}=$$
$$C_{33}\gamma_0\gamma_e\left(\frac{1}{R\gamma_0r_0}-\frac{\gamma_0e_0}{R_cr_0^2}\right)y_0+C_{33}\left(\frac{\gamma_0}{R_C}-\frac{\gamma_0^2}{r_0}\right)$$

$\dot{\varphi}_{121}$ Equation (A.8)

$$\left(-2C_\varphi V\frac{\gamma_e}{r_0^2}-C_{33}\gamma_e\left(\frac{\gamma_0^2}{r_0^2}-\frac{1}{Rr_0}-\frac{e_0\gamma_0^2}{R_cr_0^2}\right)\right)y_{12}^*-C_{23}\gamma_0\alpha_{12}^*+\left(C_\varphi+C_{11}\frac{r_0^2}{V}+C_{33}\frac{\gamma_0^2}{V}\right)\dot{\varphi}_{121}-C_\varphi\dot{\varphi}_{122}=$$
$$-C_{33}\gamma_0\gamma_e\left(\frac{1}{R\gamma_0r_0}+\frac{\gamma_0e_0}{R_cr_0^2}\right)y_0-C_{33}\left(\frac{\gamma_0}{R_C}+\frac{\gamma_0^2}{r_0}\right)$$

$\dot{\varphi}_{122}$ Equation (A.9)

$$\left(-2C_{\varphi}V\frac{\gamma_e}{r_0^2}+C_{33}\gamma_e\left(\frac{\gamma_0^2}{r_0^2}-\frac{1}{Rr_0}+\frac{e_0\gamma_0^2}{R_c r_0^2}\right)\right)y_{12}^{*}+C_{23}\gamma_0\alpha_{12}^{*}-C_{\varphi}\dot{\varphi}_{121}+\left(C_{\varphi}+C_{11}\frac{r_0^2}{V}+C_{33}\frac{\gamma_0^2}{V}\right)\dot{\varphi}_{122}=$$
$$C_{33}\gamma_0\gamma_e\left(\frac{1}{R\gamma_0 r_0}-\frac{\gamma_0 e_0}{R_c r_0^2}\right)y_0+C_{33}\left(\frac{\gamma_0}{R_c}-\frac{\gamma_0^2}{r_0}\right)$$

Notations and parameters for example vehicle

$2\overline{A}$	distance between bogies centres	18.135m
$2\overline{a}$	longitudinal distance of the springs and dampers	2m
$2a$	wheelbase of bogie	3m
$\overline{b}_0$	distance between the device levers of anti-yaw body/bogie	1.3m
C_1	modulus (magnitude) of the moment of friction in the leading wheel set damper	N.m
C_2	modulus (magnitude) of the moment of friction in the leading wheel set damper	N.m
$4Cx$	longitudinal damping coefficient of the primary suspension	variable
$4Cy$	transversal damping coefficient of the primary suspension	variable
$4\overline{Cx}$	longitudinal damping coefficient of the secondary suspension	0 N.s.m^{-1}
$4\overline{Cy}$	lateral damping coefficient of the secondary suspension	4x35000 N.s.m^{-1}
$\overline{Cz}$	vertical damping coefficient of the secondary suspension	15000 N.s.m^{-1}
C_{φ}	coefficient of résistance or damping between wheels of a wheel set	variable
$2d$	transverse distance of the springs and dampers for the primary suspension	2 m
$2\overline{d}$	transverse distance of the springs and dampers for the secondary suspension	2 m
$2d'$	transverse distance between inertia centres of wheels bearings box *(~ 2 d)*	
$2e_0$	semi-track of wheel set	1.5 m
g	gravitational acceleration	9.81m.s^{-2}
g_1	wheels relative velocity of the leading wheel set	rad.s^{-1}
g_2	wheels relative velocity of the trailing wheel set	rad.s^{-1}
$\overline{h}_0$	position of secondary plane of suspension relative to $\overline{G}$	0.880 m
$\overline{h}_1$	half height of the secondary suspension	0.210 m
$\overline{h}_2$	transverse damper position in the secondary suspension relative to secondary plan of suspension	0 m
h_0	position of primary plane of suspension relative to G_k	0.120 m
h_1	half height of the primary suspension	0m
H	vertical distance between springs points attachments of secondary suspension relative to the primary plane of suspension	0,467 m
H_1	vertical distance between transverse dampers of secondary suspension relative to the primary plane of suspension	0.670 m
H_p	distance between the lower operative point in bogie frame of the training device with the primary transverse plane of suspension	
$4Kx$	longitudinal stiffness of the primary suspension	5. MN.m^{-1}
$4Ky$	transversal stiffness of the primary suspension	7.85 MN.m^{-1}
$4Kz$	vertical stiffness of the primary suspension	4 x. 975 MN.m^{-1}

$4\overline{Kx}$	longitudinal stiffness of the secondary suspension	4 x .175 MN.m^{-1}
$4\overline{Ky}$	transversal stiffness of the secondary suspension	4 x .173 MN.m^{-1}
$4\overline{Kz}$	vertical stiffness of the secondary suspension	4 x .53 MN.m^{-1}
$\overline{K}_o$	levers stiffness of anti -yaw device between body and bogie	3.6 MN.m^{-1}
$2l$	wheel-axle set diameter	0.165m
m	mass of a wheel set	1500 kg
$\hat{m}$	mass of a wheel set box or journal bearing	250 kg
$\overline{M}$	mass of a body	43200 kg
M	mass of a bogie	3020 kg
R'	curvature radius of a rail profile	0,30 m
R	curvature radius of wheel profiles	function of γ_e
r_o	mean radius of wheel	0.45 m
s_o	longitudinal eccentricity of $\overline{G}$	0.1m
T_Z	the wheel load	
V	vehicle speed	m.s^{-1}
V_c	critical speed	m.s^{-1}
γ_0	angle of the tangential plane to the common points of contact wheel/rail with the horizontal plane when the wheel set is centred in the midline of the rail	0.025
γ_e	effective conicity	
ϑ_0	cant angle of track	6°
ϑ_d	angle of cant deficiency	
μ	coefficient of friction	0.27
ρ_y	radius of inertia of the wheel set around $\boldsymbol{G_{ki}\, y_{ki}}$ axis	
φ	increment in the angle of rotation around the axis of the wheel S_{kij} relatively to an imaginary wheel coinciding with the latter and rolling without slipping	

Subscripts

k (k = 1 for the leading truck and k =2 for the trailing truck).
i (i = 1 for the leading wheel set of a truck and i = 2 for the trailing wheel set of a truck).
j (j = 1 for the left hand side and j = 2 for the right hand side).